Danmarks Tekniske Universitet

DTU

Turbulence Modeling (46115)

Assignment 2

Turbulence Modeling of Fully Developed 1D Channel Flow

Authors

Dong Chen (s212356)
Sumukha Shridhar (s221654)
Mark van Spronsen (s223610)

November 8, 2022

Contents

1 Introduction

In the current study, the 1-D fully developed turbulent channel flow is implemented by three Reynolds Averaged Navier-Stokes (RANS) turbulence models. The results are compared with Direct Numerical Simulation (DNS) and discussed, based on which the characteristics of each model is investigated.

2 Mathematical and Numerical model of 1-D Turbulent Channel Flow

2.1 Reynolds averaged Navier-Stokes equation

The Reynolds averaged Navier-Stokes equation is derived by Reynolds decomposition of Navier-Stokes equation and is given by

$$\frac{\partial u_i}{\partial x_i} = 0 \tag{1}$$

$$\frac{D\rho u_i}{Dt} = \rho f_i - \frac{\partial p}{\partial x_i} + \frac{\partial}{\partial x_j}\left(\mu\left(\frac{\partial u_i}{\partial x_j} + \frac{\partial u_j}{\partial x_i}\right) - \rho\overline{u_i' u_j'}\right) \tag{2}$$

where $\frac{D\rho u_i}{Dt}$ is material derivative for momentum and it is zero for fully developed steady state flow. f_i, p, u_i and $\overline{u_i}$ are time averaged body force, pressure, velocity and fluctuation term respectively. The term $\rho\overline{u_i' u_j'}$ is Reynolds stress term. For 1-D fully developed channel flow, it has the relation

$$\frac{\partial u}{\partial x} = 0 \quad v, w = 0 \quad \frac{\partial P}{\partial y} = \frac{\partial P}{\partial z} = 0 \tag{3}$$

Furthermore, the effect of body force f_i is neglected.

2.2 Eddy viscosity model

In RANS turbulence model, the Reynolds stress $\rho\overline{u_i' u_j'}$ is not computed directly, but it is modeled by relating it to mean flow velocity which is inspired from Brownian motion. According to the Boussinesq hypothesis, the Reynolds stress can be approximated as

$$-\rho\overline{u_i' u_j'} = 2\mu_T S_{i,j}^* - \frac{2}{3}\rho k \delta_{i,j} \tag{4}$$

where μ_T is eddy viscosity introduced by turbulence phenomenon that is to be modeled and

$$S_{i,j}^* = \frac{1}{2}\left(\frac{\partial u_i}{\partial x_j} + \frac{\partial u_j}{\partial x_i} - \frac{1}{3}\frac{\partial u_k}{\partial x_k}\right) \tag{5}$$

and k is turbulent kinetic energy.
The eddy viscosity μ_T is modeled by various methods. Three models are implemented in this study.

2.3 prandtl mixing-length model

The eddy viscosity can be computed by the mean velocity gradient algebraically. It is assumed that the fluctuation terms can be expressed in terms of mixing length (which is analogous to the concept of mean free path in molecular dynamics)

$$v' = -l_m \left| \frac{\partial u}{\partial d} \right| \tag{6}$$

where l_m is the mixing length and d is the distance to the nearest wall. And the eddy viscosity is expressed as according to the results of dimensional analysis

$$\mu_T = \rho v' l_m = \rho \ \ l_m^2 \left| \frac{\partial u}{\partial d} \right| \tag{7}$$

where d is the distance to the nearest wall. The mixing length l_m is defined as

$$l_m = \kappa y \left(1 - e^{\frac{-y^+}{A_0^+}} \right) \tag{8}$$

where $\kappa = 0.41$ and $y^+ = \frac{y u_\tau}{\nu}$. According to Equation 3, the simplified 1D fully developed turbulence channel flow mixing length model is written as

$$0 = -\frac{\partial p}{\partial x} + \frac{\partial}{\partial y} \left(\mu + \mu_T \left(\frac{\partial u}{\partial y} \right) \right) \tag{9}$$

$$\mu_T = \rho l_m^2 \left| \frac{\partial u}{\partial y} \right| \tag{10}$$

This model is easy to implement and computationally inexpensive. It gives good prediction for flow field with simple geometry. However, as it only computes two physical quantities, detailed characteristics of turbulent flow fields with complex geometry which are described by various turbulent time and length scale, might be missing. Therefore, solving transport equations related to this time and length scale is necessary to capture all the information of turbulent flows. Based on its fast computational nature, the results computed by the Prandtl mixing length model can be used as an initial guess for the more complicated models (i.e. $k - \epsilon$ and $k - \omega$) to speed up convergence and improve the numerical stability.

2.4 Turbulence kinetic energy equation

The mean turbulence kinetic energy per unit volume of fluid is defined as the root mean squire of the velocity fluctuation

$$k = \frac{1}{2} \left(\overline{(u')^2} + \overline{(v')^2} + \overline{(w')^2} \right) \tag{11}$$

Consider Reynolds averaged Navier-Stokes from Equation 2 and multiplying both side by mean velocity u_i

$$u_i \frac{D\rho u_i}{Dt} = \rho u_i f_i - u_i \frac{\partial p}{\partial x_i} + u_i \frac{\partial}{\partial x_j} \left(\mu \left(\frac{\partial u_i}{\partial x_j} + \frac{\partial u_j}{\partial x_i} \right) - \rho \overline{u_i' u_j'} \right) \tag{12}$$

After some algebraic rearrangement, the turbulence kinetic energy equation is obtained as

$$\rho\left(\frac{\partial k}{\partial t}+u_j\frac{\partial k}{\partial x_j}\right)=\rho u_j' f_j-\rho\frac{\partial\overline{u_i'P'}}{\partial x_i}-\frac{1}{2}\rho\frac{\partial\overline{u_i'u_i'u_j'}}{\partial x_i}+\mu\frac{\partial^2 k}{\partial x_j^2}-\rho\overline{u_i'u_j'}\frac{\partial u_i}{\partial x_j}-\mu\overline{\frac{\partial u_i'}{\partial x_j}\frac{\partial u_i'}{\partial x_j}} \tag{13}$$

where the last two terms represent the turbulence kinetic energy production and dissipation term, respectively. Since the fluctuation term is modeled in the RANS equation, the original turbulence kinetic equation is written in modeled form

$$\frac{D(\rho uk)}{Dt}=\frac{\partial}{\partial x_j}\left[\left(\mu+\frac{\mu_T}{\sigma_k}\right)\frac{\partial k}{\partial x_j}\right]+\mathcal{P}-\rho\mathcal{D} \tag{14}$$

where $\mathcal{P}$ is turbulence kinetic energy production term, $\mathcal{D}$ is turbulence kinetic energy dissipation term and σ_k is closure coefficient. According to the relation in Equation 3 and the eddy viscosity model, the simplified turbulence kinetic equation is written as

$$0=\frac{\partial}{\partial y}\left[\left(\mu+\frac{\mu_T}{\sigma_k}\right)\frac{\partial k}{\partial y}\right]+\mathcal{P}-\rho\mathcal{D} \tag{15}$$

The boundary condition for turbulence kinetic energy at the wall is zero, since the fluctuation term is zero at the no-slip wall.

2.5 $k-\epsilon$ turbulence model

The $k-\epsilon$ turbulence model is a two equation model of the turbulence kinetic energy equation (k-equation) Equation 14 and the rate of dissipation of turbulent kinetic energy (ϵ equation)

$$\frac{D(\rho u\epsilon)}{Dt}=\frac{\partial}{\partial x_j}\left[\left(\mu+\frac{\mu_T}{\sigma_\epsilon}\right)\frac{\partial \epsilon}{\partial x_j}\right]+C_{\epsilon,1}\frac{\epsilon}{k}\mathcal{P}-C_{\epsilon,2}\rho\frac{\epsilon^2}{k} \tag{16}$$

According to the relation in Equation 3 and eddy viscosity model, the simplified ϵ equation can be written as

$$0=\frac{\partial}{\partial y}\left[\left(\mu+\frac{\mu_T}{\sigma_\epsilon}\right)\frac{\partial k}{\partial y}\right]+C_{\epsilon,1}\frac{\epsilon}{k}\mathcal{P}-C_{\epsilon,2}\rho\frac{\epsilon^2}{k} \tag{17}$$

The production term $\mathcal{P}$ and dissipation term $\mathcal{D}$ are expressed as

$$\mathcal{P}=\rho\overline{u'v'}\frac{\partial u}{\partial y}\quad \mathcal{D}=\epsilon \tag{18}$$

and the eddy viscosity is expressed in terms of k and ϵ

$$\mu_T=\rho C_\mu\frac{k^2}{\epsilon} \tag{19}$$

where the closure coefficients for $k-\epsilon$ model are

$$C_{\epsilon,1}=1.44\quad C_{\epsilon,2}=1.92\quad C_\mu=0.09\quad \sigma_k=1.0\quad \sigma_\epsilon=1.3 \tag{20}$$

Literature and experiments indicate that the $k-\epsilon$ model over-predicts the eddy viscosity in near wall region. Therefore the damping functions is necessary to give simulation results that

are in good agreement with the experimental results. The Van Driest damping function is applied in the current study to damp the eddy viscosity near the wall predicted by $k-\epsilon$ model

$$f_\mu = \left(1 - e^{\frac{-y^+}{A^+}}\right)^2 \tag{21}$$

where A^+ is the model constant, and u_τ is the frictional velocity that is used to define Reynolds number based on frictional velocity

$$Re_\tau = \frac{u_\tau h}{\nu} \tag{22}$$

where h is the full channel height. Consequently, the damped eddy viscosity is expressed as

$$\mu_T = f_\mu \rho C_\mu \frac{k^2}{\epsilon} \tag{23}$$

According to the relation in Equation 3, the $k-\epsilon$ model for 1D fully developed channel flow is expressed as

$$0 = \frac{\partial}{\partial y}\left[\left(\mu + \frac{\mu_T}{\sigma_k}\right)\frac{\partial k}{\partial y}\right] + \mathcal{P} - \rho\epsilon \tag{24}$$

$$0 = \frac{\partial}{\partial y}\left[\left(\mu + \frac{\mu_T}{\sigma_\epsilon}\right)\frac{\partial \epsilon}{\partial y}\right] + C_{\epsilon,1}\frac{\epsilon}{k}\mathcal{P} - C_{\epsilon,2}\rho\frac{\epsilon^2}{k} \tag{25}$$

and the production term of turbulence kinetic energy is expressed as

$$\mathcal{P} = \mu_T \left(\frac{\partial u}{\partial y}\right)^2 \tag{26}$$

At the wall $y = 0$, the fluctuation velocity is zero, and the dissipation term is expressed as

$$\epsilon_{y=0} = \nu\left(\frac{\partial u_i'}{\partial x_j}\right)^2 \tag{27}$$

$$= \nu\left(\frac{\partial}{\partial x_j}\left(u_i'\frac{\partial u_i'}{\partial x_j}\right) - u_j'\frac{\partial^2 u_i'}{\partial x_j^2}\right) \tag{28}$$

$$= \nu\frac{\partial}{\partial x_j}\left(\frac{1}{2}\frac{\partial u_i'^2}{\partial^2 x_j}\right) = \nu\frac{\partial^2 k}{\partial x_j^2} \tag{29}$$

2.6 $k-\omega$ SST (Shear Stress Transport) turbulence model

The specific turbulence dissipation rate is defined as

$$\omega = \frac{\epsilon}{C_\mu k} \quad C_\mu = 0.09 \tag{30}$$

Substitute Equation 30 into Equation 16 to obtain

$$\frac{D(\rho u\omega)}{Dt} = \frac{\partial}{\partial x_j}\left[(\mu + \mu_T\sigma_\omega)\frac{\partial \omega}{\partial x_j}\right] + \frac{\gamma}{\nu_t}\mathcal{P} - \beta\rho\omega^2 + 2\frac{\rho\sigma_{\omega,2}}{\omega}\frac{\partial k}{\partial x_j}\frac{\partial \omega}{\partial x_j} \tag{31}$$

where there exists an additional term

$$2\frac{\rho\sigma_{\omega,2}}{\omega}\frac{\partial k}{\partial x_j}\frac{\partial \omega}{\partial x_j} \tag{32}$$

When Equation 64 is neglected, the above equation along with the Equation 14 is the standard $k-\omega$ turbulence model, and when Equation 64 remains, the above equation along with the Equation 14 is standard $k-\epsilon$ turbulence model. In engineering applications, it is favorable that no damping function is needed near the wall. This is necessary to cope with the variety of pressure gradient conditions so that it has a good near wall behavior. This is the advantage of the $k-\omega$ model with respect to the $k-\epsilon$ model. Furthermore, the model should be less sensitive to the free stream inlet boundary condition, which is the advantage of the $k-\epsilon$ model with respect to the $k-\omega$ model. As a consequence, the $k-\omega$ SST model is proposed for the purpose that a smooth transition is realized between the near wall region ($k-\omega$ model) and the region away from the wall ($k-\epsilon$). The blending function F_1 that is used to transit this two models is introduced

$$F_1 = \tanh\left(arg_1^4\right) \tag{33}$$

$$\arg_1 = \min\left[\max\left(\frac{\sqrt{k}}{\beta^*\omega d}\right), \frac{4\rho\sigma_{\omega,2}k}{CD_{k\omega}d^2}\right] \tag{34}$$

$$\mathrm{CD}_{k\omega} = \max\left(2\rho\sigma_{\omega,2}\frac{1}{\omega}\frac{\partial k}{\partial x_j}\frac{\partial \omega}{\partial x_j}, 10^{-20}\right) \tag{35}$$

where d is the distance to the nearest wall, such that Equation 36 can be switched between $k-\epsilon$ ($F_1=0$) and $k-\omega$ ($F_1=1$) smoothly.

$$\frac{D(\rho u\omega)}{Dt} = \frac{\partial}{\partial x_j}\left[\left(\mu+\mu_T\sigma_\omega\right)\frac{\partial \omega}{\partial x_j}\right] + \frac{\gamma}{\nu_t}\mathcal{P} - \beta\rho\omega^2 + 2(1-F_1)\frac{\rho\sigma_{\omega,2}}{\omega}\frac{\partial k}{\partial x_j}\frac{\partial \omega}{\partial x_j} \tag{36}$$

The closure coefficient is computed by the blending function

$$\phi = F_1\phi_1 + (1-F_1)\phi_2 \tag{37}$$

where ϕ_1 and ϕ_2 are the closure coefficients defined as

$$\sigma_{k,1} = 0.85 \quad \sigma_{\omega,1} = 0.5 \quad \beta_1 = 0.0075 \quad \gamma_1 = \frac{5}{9} \tag{38}$$

$$\sigma_{k,2} = 1.0 \quad \sigma_{\omega,2} = 0.856 \quad \beta_2 = 0.0828 \quad \gamma_2 = 0.44 \tag{39}$$

The eddy viscosity is computed from

$$\mu_T = \frac{\rho a_1 k}{\max(a1\omega, \Omega F_2)} \tag{40}$$

where $a_1 = 0.31$, F_2 is defined as

$$F_2 = \tanh\left(arg_2^2\right) \quad arg_2 = \max\left(2\frac{\sqrt{k}}{\beta^*\omega d}, \frac{500\nu}{d^2\omega}\right) \tag{41}$$

and $\Omega = \sqrt{2W_{ij}W_{ij}}$ is the vorticity magnitude where

$$W_{ij} = \frac{1}{2}\left(\frac{\partial u_i}{\partial x_j} - \frac{\partial u_j}{\partial x_i}\right) \tag{42}$$

The turbulence kinetic energy production term $\mathcal{P}$ is limited in magnitude and is replaced by

$$\mathcal{P} = \min(\mathcal{P}, 20\beta^*\rho\omega k) \tag{43}$$

The boundary condition at the wall are

$$k_{wall} = 0 \quad \omega_{wall} = 10\frac{6\nu}{\beta_1(\Delta d_1)^2} \tag{44}$$

According to the Equation 3, the simplified $k-\omega$ SST model for 1-D turbulent fully developed channel flow is written as

$$0 = \frac{\partial}{\partial y}\left[(\mu + \mu_T\sigma_k)\frac{\partial k}{\partial y}\right] + \mathcal{P} - \beta^*\rho\omega k \tag{45}$$

$$0 = \frac{\partial}{\partial y}\left[(\mu + \mu_T\sigma_\omega)\frac{\partial \omega}{\partial y}\right] + \frac{\gamma}{\mu_T}\mathcal{P} - \beta\rho\omega^2 + 2(1-F_1)\frac{\rho\sigma_{\omega,2}}{\omega}\frac{\partial k}{\partial y}\frac{\partial \omega}{\partial y} \tag{46}$$

2.7 Law of the wall

For turbulent boundary layers, the shear stress is composed of two terms and for small y^+, the Reynolds stress is negligible. Therefore

$$\tau = \mu\frac{du}{dy} + \left(-\rho\overline{u'v'}\right) \approx \mu\frac{du}{dy} \tag{47}$$

and the relation can be derived for small y^+

$$\tau \approx \mu\frac{du}{dy} \quad u = \frac{u_\tau^2}{\nu}y \tag{48}$$

$$u = u_\tau y^+ \tag{49}$$

Experimental results show that it agrees well for $y^+ < 5$, in which it is called viscous sub-layer. This is the theory for grid spacing of turbulence modelling that in order to capturing the information of the viscous sub-layer, the first grid should be less than $\Delta y_1^+ < 5$. As y^+ gets larger, the viscous term $\mu\frac{du}{dy}$ becomes negligible.

$$\tau \approx \left(-\rho\overline{u'v'}\right) \tag{50}$$

The mean velocity profile can be obtained from dimensional analysis. The mean velocity u can be expressed as a function

$$u = F(\tau, y, \mu, \rho) \approx F(\tau, y, \rho) \tag{51}$$

since the viscous effect is minus, and taking the space derivative of it

$$0 = \Psi\left(\frac{du}{dy}, \tau, y, \rho\right) \tag{52}$$

From dimensional analysis, Equation 52 is rewritten as

$$0 = \Psi\left(\frac{du}{dy}\frac{1}{\frac{u_\tau}{y}}\right) \tag{53}$$

therefore, it can be concluded that the term inside the bracket is a constant.

$$\frac{du}{dy}\frac{1}{\frac{u_\tau}{y}} = A \tag{54}$$

$$\frac{du}{dy} = Au_\tau\frac{1}{y} \tag{55}$$

Integrating Equation 55

$$u = u_\tau(A\ln(y) + B) \tag{56}$$

where A and B are universals constant determined by experimental observation. For a hydraulic smooth wall $A = 2.5$ and $B = 5.1$. The Equation 56 is in good agreement with the observation for $30 < y^+ < 500$ where it is called log-law region. In the region $5 < y^+ < 30$ where both expressions fails to describe the mean velocity profile, it is called buffer layer.
The above derived relation is called the law of the wall, which is used to validate the correctness of the implemented model and is to be applied for high quality mesh generation.

2.8 Numerical scheme

The Prandtl mixing length model Equation 10, the $k-\epsilon$ model Equation 29 and $k-\omega$ SST model Equation 46 for fully developed turbulent 1-D channel flow are solved by using a finite difference scheme. Since the convective term is not considered in the current case, second order central difference scheme is applied to achieve relatively high accuracy while there is no risk of non-physical numerical oscillation due to the convection term. The detailed finite difference method discretization scheme is elaborated in assignment 1 and is not repeated here. For the non-linear equation, Newton's iterative method and Jacobi iterative method for linearized non-linear discretized equation are implemented in the current study. Since the fully developed channel flow is symmetric about the center-line, the computational domain is selected to be half channel for the computational efficiency.

Jacobi iteration method

The well posed discretized system is written as

$$\boldsymbol{L\phi} = \boldsymbol{b} \tag{57}$$

where $\boldsymbol{\phi}$ is the fluid field value, $\boldsymbol{L}$ is the linear operator and $\boldsymbol{b}$ is the right-hand side term which contains the value from the last iteration and includes nonlinear term. The Jacobi iteration method starts with proper initial guessing (could be results from the Prandtl mixing length model), and consequently obtains each fluid field value by solving corresponding discretized system. Finally, each fluid field value is updated until the solution converges.

Newton's iteration method

The discretized non-linear equation is to be expressed as

$$\boldsymbol{G}(\boldsymbol{\phi}) = 0 \tag{58}$$

for Newton's iterative method. It starts with guessing an initial value. The update of each iteration is derived by Taylor expansion:

$$\boldsymbol{G}(\boldsymbol{\phi}^{k+1}) \approx \boldsymbol{G}(\boldsymbol{\phi}^{k}) + \boldsymbol{G}'(\boldsymbol{\phi}^{k})(\boldsymbol{\phi}^{k+1} - \boldsymbol{\phi}^{k}) \tag{59}$$

where $\boldsymbol{G}'$ is expressed by the Jacobian matrix of the discretized system of equation

$$\boldsymbol{J}_{ij}(\boldsymbol{\phi}^{k}) = \frac{\partial}{\partial \boldsymbol{\phi}_j}\boldsymbol{G}_i(\boldsymbol{\phi}) \tag{60}$$

consequently the update term δ^k can be calculated by linear system

$$\boldsymbol{J}(\boldsymbol{\phi}^{k})\delta^{k} = -\boldsymbol{G}(\boldsymbol{\phi}^{k}) \tag{61}$$

The relaxation factor β can be applied to under-relax the iteration step of both aforementioned iterative solvers to avoid the divergence, since the turbulence model is non-linear and could be numerically unstable

$$\boldsymbol{\phi}_{new} = (1-\beta)\boldsymbol{\phi}_{old} + \beta\phi_{old} \tag{62}$$

where $\beta \in (0, 1)$.
According to the law of the wall, the first grid spacing $\Delta y_1^+ = 1$ is selected for the current study. Non-uniform grid is applied.
The stopping criterion for iterative solver in the current study is that the norm of residual $norm(\boldsymbol{R}) \leq 10^{-10}$.

3 Implemented Turbulence Model and Results

The the three models are implemented by MATLAB. The simulated results are compared with the Direct Numerical Simulation (DNS) [3], which computes all the scale of the fluid flow thus has the highest accuracy. And the mean velocity is plotted in the $\log(y^+)$ scale for the convenience of validating against the law of the wall.

3.1 Computed results of Prandtl mixing length model

The Prandtl model is implemented and the computed velocity profile in $u - \log(y^+)$ scale are shown in Figure 1 to Figure 4. It is shown that the Prandtl mixing length model has a comparatively good accuracy in flow field with moderate Re_τ among the four Reynolds number. While its accuracy is low at low Re_τ for predicting the fluid flow in log-law region. The reason is that the mixing length is accurate for large comparatively large y^+. While as Re_τ large enough, the mixing length model has large error at high y^+ location. The reason behind that is that the mixing length hypothesis can only accurately describe the physical phenomenon at near wall region, and the flow field condition becomes so complicated that mixing length is not

capable of capture all the information. That means the accuracy for Prandtl mixing length model is low for flow with complex geometry and the region away from the wall.

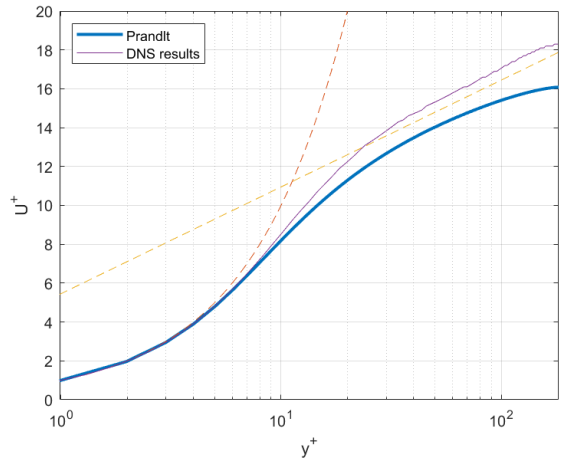

Figure 1: Mean velocity u for $Re_\tau = 182$

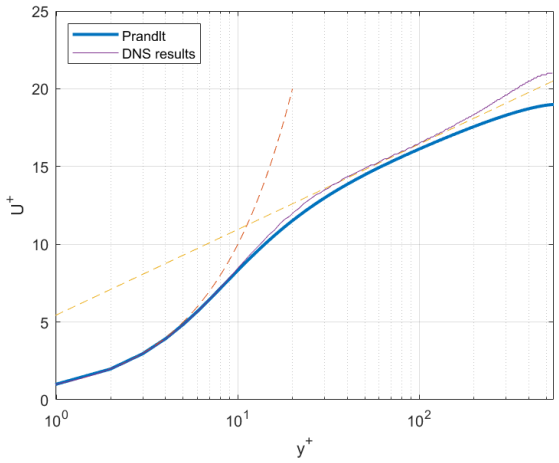

Figure 2: Mean velocity u for $Re_\tau = 550$

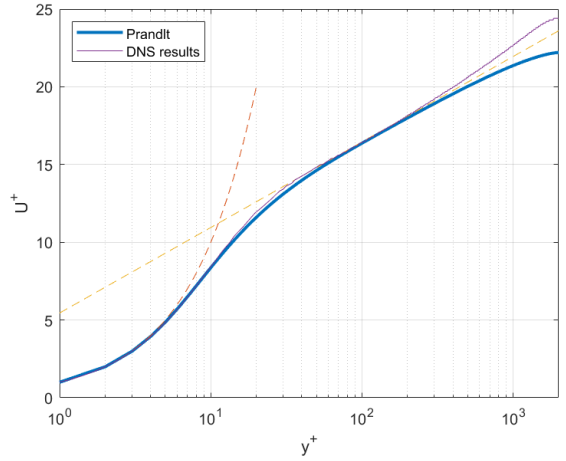

Figure 3: Mean velocity u for $Re_\tau = 2000$

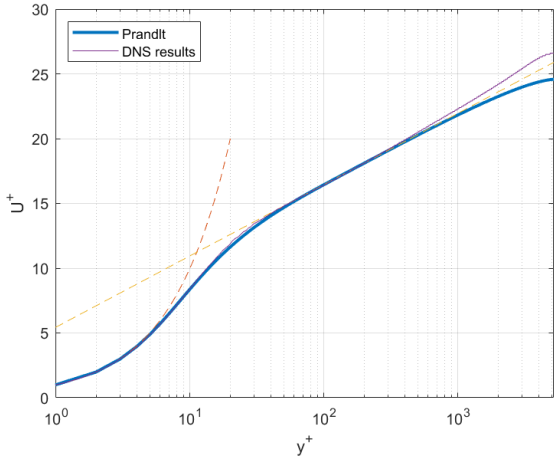

Figure 4: Mean velocity u for $Re_\tau = 5200$

3.2 Computed results of $k - \epsilon$ model

The simulation results of the $k - \epsilon$ model are shown in figures from Figure 5 to Figure 7, and the effect of damping function is also investigated.
It is observed that the DNS results are in good agreement with the law of the wall, that means it can be adopted as the bench mark to test the correctness of the implemented model to some extent. The compared results show that the error of $k - \epsilon$ model makes the computational results non-physical, because the term

$$2\frac{\rho\sigma_{\omega,2}}{\omega}\frac{\partial k}{\partial x_j}\frac{\partial \omega}{\partial x_j} \tag{63}$$

over-predicts the eddy viscosity μ_T at the near wall region compared with the results of other models as Figure 23 indicates. As a consequence, the shear stress near wall is over-predicted

by original $k-\epsilon$ model therefore the velocity of the whole computational domain is under-predicted, from which it can be concluded that the damping function is vital in $k-\epsilon$ model for fluid flow with slightly higher Reynolds number. Even if the damping function is implemented for $k-\epsilon$ model, the velocity predicted by $k-\epsilon$ at large y^+ deviates from theoretical and DNS results due to the error introduced by damping function.

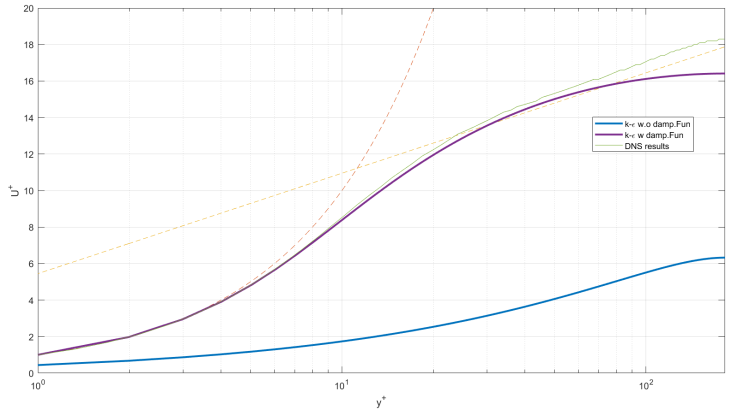

Figure 5: Mean velocity profile in $u - \log(y^+)$ plot, $Re_\tau = 180$

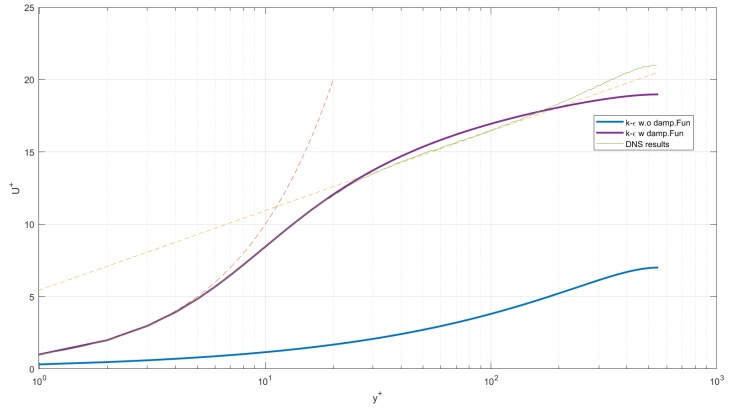

Figure 6: Mean velocity profile in $u - \log(y^+)$ plot, $Re_\tau = 550$

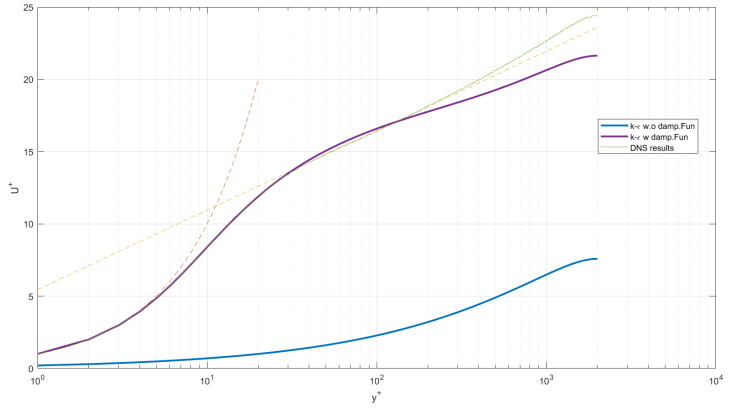

Figure 7: Mean velocity profile in $u - \log(y^+)$ plot, $Re_\tau = 2000$

The other turbulence quantities Reynolds stress $\rho\overline{u_i' u_j'}$, turbulence kinetic energy k and the rate of dissipation of turbulence kinetic energy ϵ are shown in Figure 8 to Figure 17 for the case of $Re_\tau = 182$. The Reynolds number effect changes these values quantitatively but not

qualitatively within the range of the current study ($Re_\tau = 180 - 2000$). It is observed from Figure 8 that the velocity profile is not parabolic as is in laminar case because turbulent flow is characterized by strong mixing of momentum such that the momentum near the wall is supplemented by the free stream much more than that of laminar flow.

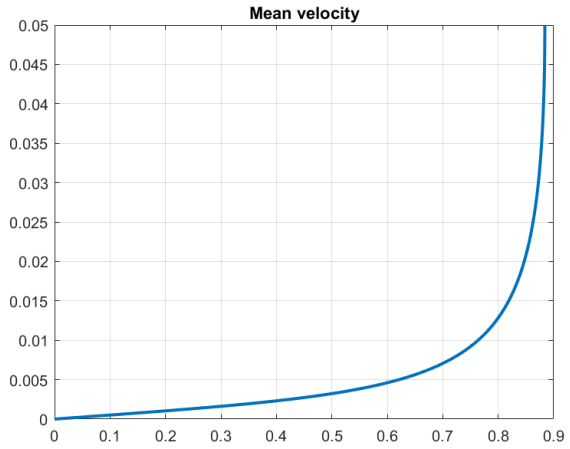

Figure 8: Mean velocity u in normal scale

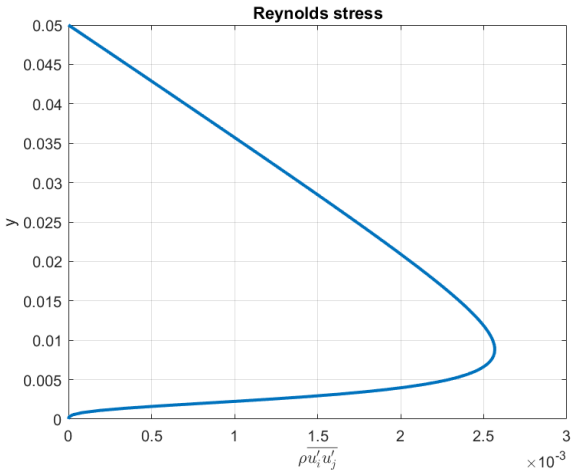

Figure 9: Reynolds stress

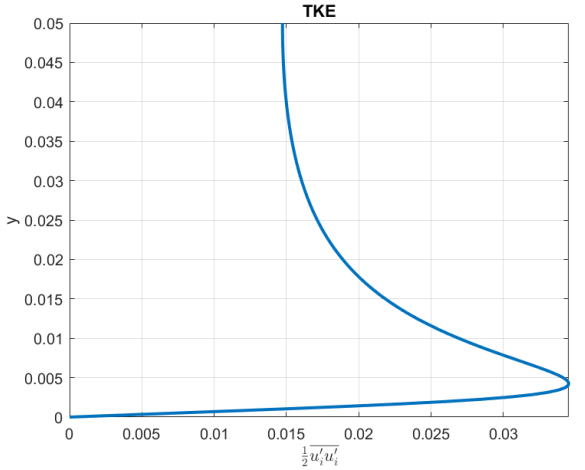

Figure 10: Turbulence kinetic energy

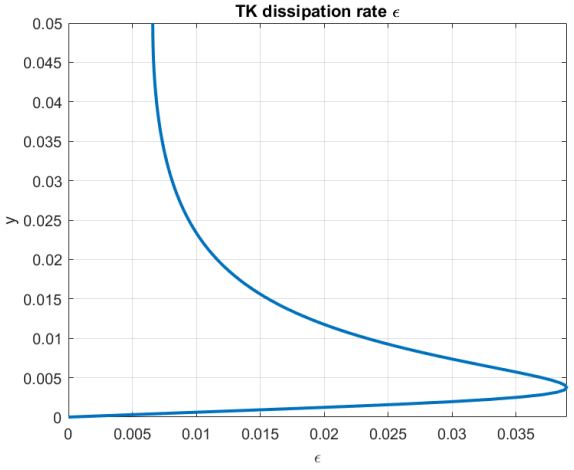

Figure 11: Rate of TKE dissipation ϵ

While the $k-\epsilon$ model behaves much better with the damping function, damping function makes the model fails to capture the flow field with various pressure gradient condition, especially for adverse pressure gradient where separation need to be considered. Therefore, a more robust model for describing the turbulent flow is implemented.

3.3 Computed results of $k-\omega$ SST model

As is aforementioned, the term in specific rate of dissipation rate equation ω

$$2\frac{\rho\sigma_{\omega,2}}{\omega}\frac{\partial k}{\partial x_j}\frac{\partial \omega}{\partial x_j} \tag{64}$$

under-predicts the ϵ in the near wall region such that the eddy viscosity is over predicted. While if this term is neglected, which is standard $k-\omega$ model does, the model becomes free stream

dependent since the missing terms might be important in flow field away from the wall. The essence of $k-\omega$ SST model is to blend $k-\omega$ model in the near wall region and $k-\epsilon$ model in the region away from the wall. As a result, no damping function is required so that the model predict the flow field accurately for various pressure condition and the error due to the damping function is eliminated; the model is free stream independent so it gives proper prediction for the flow away from the wall. As is observed in Figure 12 to Figure 7.

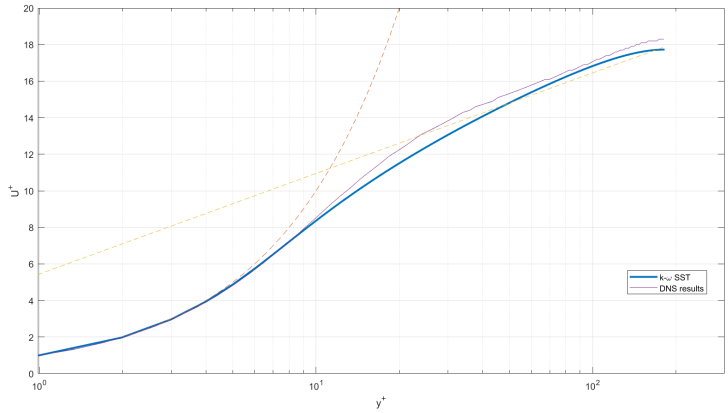

Figure 12: Mean velocity profile in $u - \log(y^+)$ plot, $Re_\tau = 180$

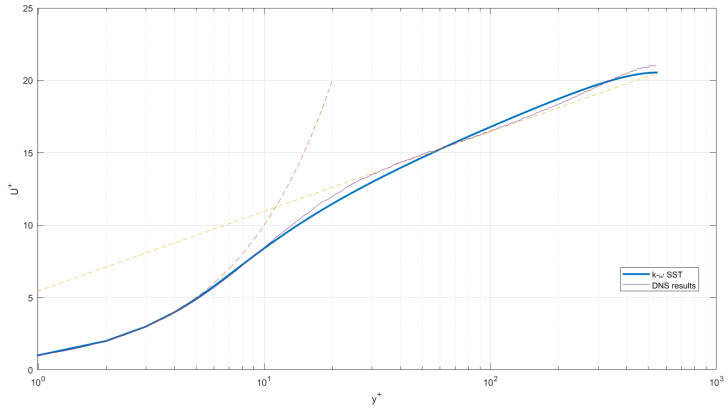

Figure 13: Mean velocity profile in $u - \log(y^+)$ plot, $Re_\tau = 550$

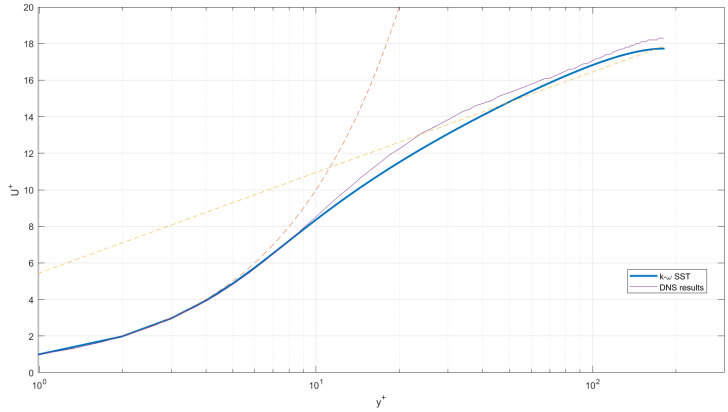

Figure 14: Mean velocity profile in $u - \log(y^+)$ plot, $Re_\tau = 2000$

Compared with the result of $k-\omega$ SST model with that of $k-\epsilon$ model, it is observed that the $k-\omega$ SST model gives more accurate prediction for large y^+ than that of $k-\epsilon$ model which

is in accordance with the discussion above. The other turbulence quantities Reynolds stress $\rho\overline{u_i'u_j'}$, turbulence kinetic energy k, specific rate of dissipation ω, and rate of dissipation ϵ for $Re_\tau = 182$ are shown in Figure 15 to Figure 18. The Reynolds stress is approximately the same as that of $k-\epsilon$ model. The turbulence kinetic energy k predicted by $k-\omega$ SST model is smaller than that predicted by $k-\epsilon$ and the rate of k dissipation is larger than that predicted by $k-\omega$ SST model in the near wall region. Consequently, the eddy viscosity predicted is smaller than that predicted by $k-\epsilon$ model in near wall region according to Equation 40.

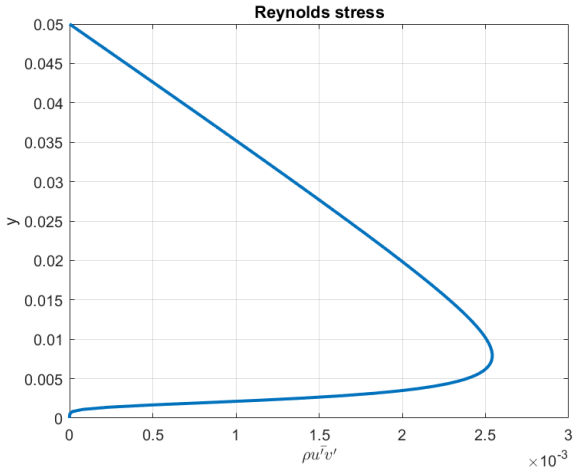

Figure 15: Reynolds stress

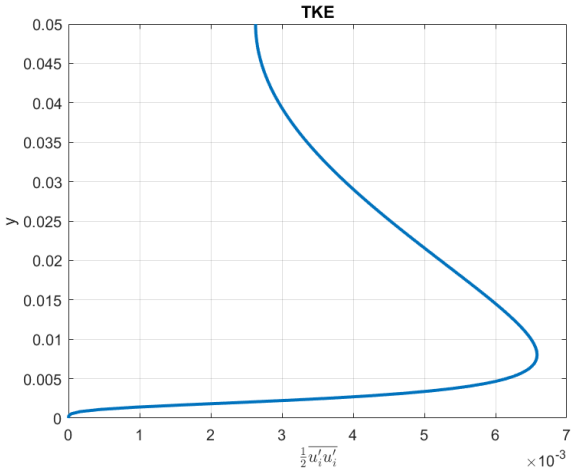

Figure 16: Turbulence kinetic energy

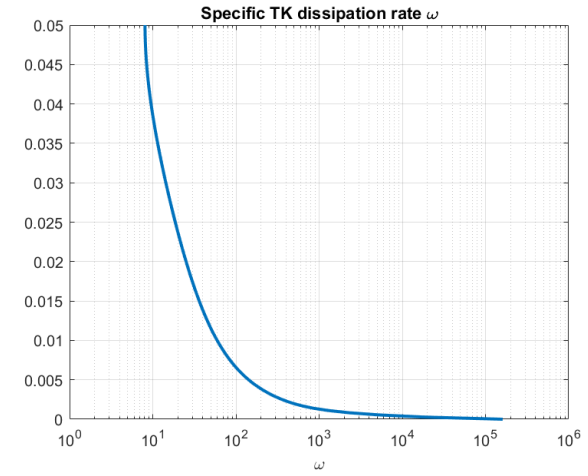

Figure 17: Specific rate of TKE dissipation ω

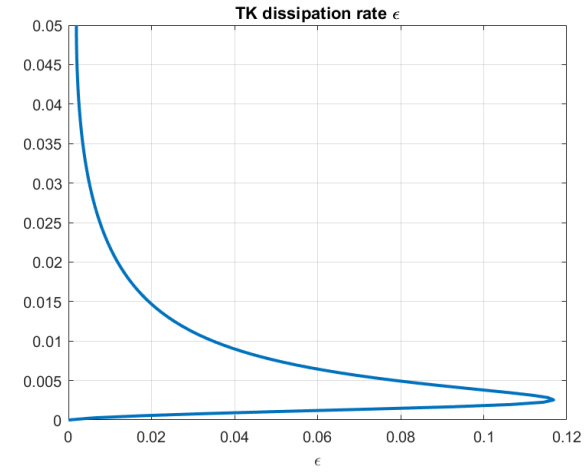

Figure 18: Rate of TKE dissipation ϵ

3.4 Comparison of $k-\epsilon$ and $k-\omega$ SST model

According to the DNS results, the law of the wall shows good agreement for $108 \leq Re_\tau \leq 2003$ [2]. Both of the model give the predictions show small discrepancy with the DNS results, while the error is acceptable and the solutions still show good physical sense. The accuracy of $k-\omega$ SST model is superior to that of $k-\epsilon$ with damping function for high y^+ region because there is no damping function that introduces error. While in the region between buffer layer and log-law region, the accuracy of $k-\omega$ SST is inferior than that of $k-\epsilon$ due to the error introduced by blending function. The convergence history of $k-\epsilon$ and $k-\omega$ SST model are shown in

Figure 19 and Figure 20. Due to the fact that $k-\omega$ SST model requires no damping function incorporated, the connection between parameters is smaller than that of $k-\epsilon$ model. Therefore the stiffness of discretized system of $k-\omega$ SST model is smaller. Consequently, the numerical stability and iteration required to converge is less than that of $k-\epsilon$ model, as is indicated in the figures, the $k-\omega$ SST model has less oscillation during the iteration process and has much less iteration steps than that of $k-\epsilon$ model. Figure 21 shows that the accuracy at high Re_τ computed by $k-\omega$ SST model is still high which means it is a feasible solver for higher Re_τ, while the computational performance of $k-\epsilon$ with damping function is poor so that the result is not presented here. The $k-\omega$ SST model converges fast at Re_τ as high as 8000 as is shown in Figure 22 and gives the prediction that in good agreement with the law of the wall. The comparison indicates that $k-\omega$ SST model is much more robust than $k-\epsilon$ model.
The other important source of deviation from the DNS results and the law of wall of both of this two model is the modelling error. The DNS benchmark is computed in 3D domain where velocity fluctuation in all direction is considered. But for the 1D case in the current study, only u' and v' is considered.

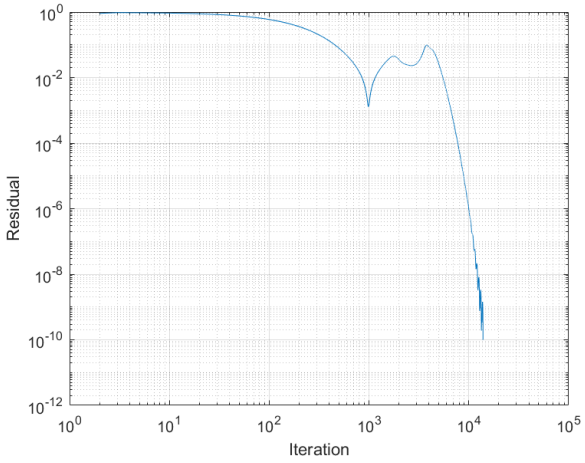

Figure 19: Convergence history of $k-\epsilon$ model, $Re_\tau = 2000$

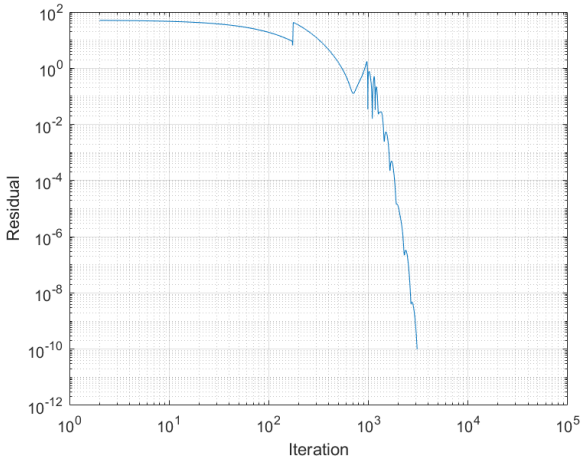

Figure 20: Convergence history of $k-\omega$ SST model, $Re_\tau = 2000$

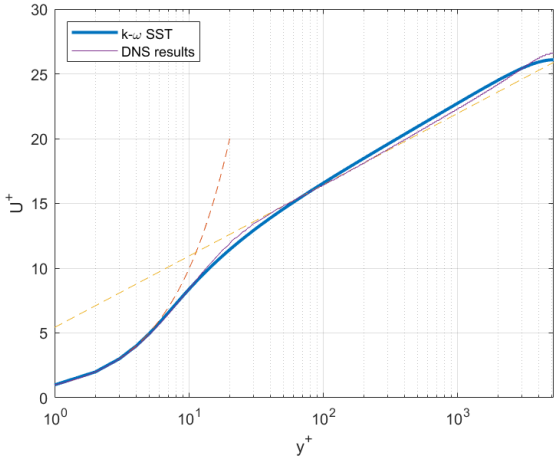

Figure 21: Mean velocity profile in $u-\log(y^+)$ plot for $k-\omega$ SST, $Re_\tau = 5200$

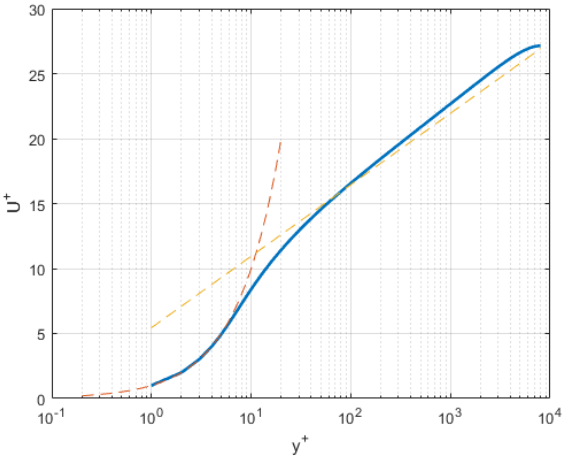

Figure 22: Mean velocity profile in $u-\log(y^+)$ plot for $k-\omega$ SST, $Re_\tau = 8000$

3.5 Computed eddy viscosity

The nature of the eddy viscosity turbulence modelling is to model the eddy viscosity μ_T, which are shown in Figure 23 for the computed results of the model studied by the current study. As is seen in the figure, the non-parabolic mean velocity profile is due to non-constant eddy viscosity and it increases as the distance from the wall increases. The eddy viscosity is larger than the molecular viscosity away from the wall which means the turbulence intensity is large away from the wall. The μ_T predicted by $k-\epsilon$ model is much larger than that predicted by $k-\omega$ SST model at near wall region, thus less accurate for $k-\epsilon$ model without damping function, which could be modified by the implementation of damping function as indicated in the figure. It is also noticeable that the eddy viscosity predicted by mixing length model fails to express the physical meaning in the center-line due to its definition.

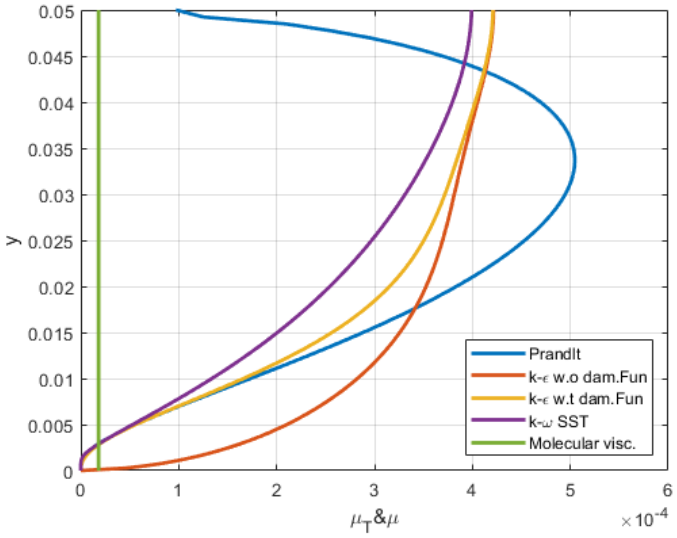

Figure 23: Eddy viscosity μ_T distribution for computed results of various model, $Re_\tau = 180$

4 Conclusions

In the current study, three eddy viscosity turbulence models, Prandtl mixing length model, $k-\epsilon$ model and $k-\omega$ SST model are studied and implemented for 1-D turbulent fully developed channel flow. The Jacobi iteration method for nonlinear system of equation and Newton iterative method are adopted to solve the discretized finite difference equation.

Results shows that for such simple flow geometry, Prandtl mixing length model gives good prediction for flow with simple geometry and moderate Re_τ in the viscous sub-layer and log-law region with lowest computational cost. While due to the fact that none of the turbulence scale is modeled by Prandtl mixing length model, its accuracy for complex flow geometry is low.

For $k-\epsilon$ model, the error of the solution is so large that it has poor physical meaning because it over-predicts the eddy viscosity. To cope for this problem, damping function is applied to lower the eddy viscosity in the near wall region. While the accuracy is improved with damping function incorporated, the computational performance of $k-\epsilon$ model with damping function is inferior since the implementation of damping function increases the stiffness of the discretized

system. Besides, for flow away from the wall, damping function could also introduces error. Because the error is large in the near wall region, $k-\epsilon$ model gives inaccurate prediction for complex pressure condition such as separation where adverse pressure gradient occurs. The advantage of the $k-\epsilon$ equation is that it is free stream independent.
One of the solution to conserve the advantage of free stream independence of $k-\epsilon$ model and to eliminate the requirement of damping function which is the advantage of $k-\omega$ model is $k-\omega$ SST model. It blends this two models by a blending function that solves for $k-\omega$ model in the near wall region and solves for $k-\epsilon$ model in the free stream that is away from the wall. Results shows $k-\omega$ SST gives a better solution and has more efficient computational performance than $k-\epsilon$.

References

[1] Menter, F. R. (August 1994). "Two-Equation Eddy-Viscosity Turbulence Models for Engineering Applications". AIAA Journal. 32 (8): 1598-1605

[2] Absi, Rafik (2009), "A simple eddy viscosity formulation for turbulent boundary layers near smooth walls", Comptes Rendus Mécanique, 337 (3): 158-165

[3] `https://turbulence.oden.utexas.edu/`